Development 134, 19-29 (2007) doi:10.1242/dev.02709

A Zn-finger/FH2-domain containing protein, FOZI-1, acts redundantly with CeMyoD to specify striated body wall muscle fates in the *Caenorhabditis elegans* postembryonic mesoderm

Nirav M. Amin, Kejin Hu, David Pruyne, Dino Terzic, Anthony Bretscher and Jun Liu*

Striated muscle development in vertebrates requires the redundant functions of multiple members of the MyoD family. Invertebrates such as *Drosophila* and *Caenorhabditis elegans* contain only one MyoD homolog in each organism. Earlier observations suggest that factors outside of the MyoD family might function redundantly with MyoD in striated muscle fate specification in these organisms. However, the identity of these factors has remained elusive. Here, we describe the identification and characterization of FOZI-1, a putative transcription factor that functions redundantly with CeMyoD (HLH-1) in striated body wall muscle (BWM) fate specification in the *C. elegans* postembryonic mesoderm. *fozi-1* encodes a novel nuclear-localized protein with motifs characteristic of both transcription factors and actin-binding proteins. We show that FOZI-1 shares the same expression pattern as CeMyoD in the postembryonic mesodermal lineage, the M lineage, and that *fozi-1*-null mutants exhibit similar M lineage-null defects to those found in animals lacking CeMyoD in the M lineage (e.g. loss of a fraction of M lineage-derived BWMs). Interestingly, *fozi-1*-null mutants with a reduced level of CeMyoD lack most, if not all, M lineage-derived BWMs. Our results indicate that FOZI-1 and the Hox factor MAB-5 function redundantly with CeMyoD in the specification of the striated BWM fate in the *C. elegans* postembryonic mesoderm, implicating a remarkable level of complexity for the production of a simple striated musculature in *C. elegans*.

KEY WORDS: *fozi-1*, Formin, FH2 domain, Zinc finger, Mesoderm, Cell fate specification, M lineage, Body wall muscle, HLH-1, CeMyoD, MAB-5, CEH-20, Myogenesis

INTRODUCTION

Mesodermal development is a complex multistep process in which the pluripotent precursor cells become increasingly specialized to form specific cell types. This process requires a coordination of multiple transcriptional pathways and cellular signaling mechanisms. The *Caenorhabditis elegans* postembryonic mesodermal lineage, the M lineage, allows us to study these mechanisms at single cell resolution. The M lineage arises from a single blast cell, the M mesoblast, which is born during embryogenesis and remains dormant until the larva hatches (Sulston and Horvitz, 1977; Sulston et al., 1983). During larval development this pluripotent blast cell undergoes a series of reproducible divisions to give rise to all of the postembryonically derived, non-gonadal mesodermal cells in the animal (Sulston and Horvitz, 1977). In hermaphrodites, the M mesoblast undergoes a series of divisions to give rise to a total of 18 cells. Fourteen of these cells become striated body wall muscles (BWMs) and two become non-muscle coelomocytes (CCs) (Sulston and Horvitz, 1977) (Fig. 1). The remaining two cells become sex myoblasts (SMs), which migrate to the presumptive vulval region and further proliferate to give rise to eight vulval muscles and eight uterine muscles (Sulston and Horvitz, 1977) (Fig. 1).

Previous studies have identified a number of transcriptional regulators that are required for proper CC and BWM fate specification in the M lineage. These factors include the Hox factor MAB-5 and its co-factor CEH-20 (Liu and Fire, 2000), the HMX homeodomain protein MLS-2 (Jiang et al., 2005), the MyoD homolog HLH-1 (Harfe et al., 1998a) and the Twist ortholog HLH-8 (Harfe et al., 1998b). MAB-5 and CEH-20 directly activate expression of HLH-8 (Liu and Fire, 2000), while MLS-2 regulates the expression of CeMyoD (HLH-1) in the M lineage (Jiang et al., 2005). Among these transcriptional regulators, HLH-1 is required specifically for BWM and CC fate specification in the M lineage (Harfe et al., 1998a). Lack of HLH-1 in the M lineage does not cause any early defects within the lineage. Instead, it causes stochastic cell fate transformations of several BWMs and the two CCs to SMs (Harfe et al., 1998a). HLH-1 is the only member of the myogenic basic helix-loop-helix (bHLH) family in *C. elegans* (Krause et al., 1990). Its requirement for BWM fate specification in the M lineage suggests a functional similarity between HLH-1 and the vertebrate myogenic bHLH proteins (Pownall et al., 2002). However, as only a subset of the BWM cells are transformed in mutant animals completely lacking HLH-1 in the M lineage, additional factors must exist for the proper specification of BWM fates.

To identify these additional factors, we screened for mutants with defects in the M lineage (*mesodermal lineage specification*, or *mls*, mutants). In this paper, we describe one gene, *fozi-1* (*formin zinc finger protein-1*), that was identified through these screens. *fozi-1* encodes a novel nuclear protein with motifs characteristic of transcription factors and actin-binding proteins. Like *hlh-1*, *fozi-1* is expressed in the M lineage and functions within the M lineage for proper CC and BWM cell fate specification. We show that FOZI-1 and the Hox factor MAB-5 function redundantly with HLH-1 to specify BWM fate in the M lineage.

Department of Molecular Biology and Genetics, Cornell University, Ithaca, NY 14853, USA.

*Author for correspondence (e-mail: JL53@cornell.edu)

Accepted 20 October 2006

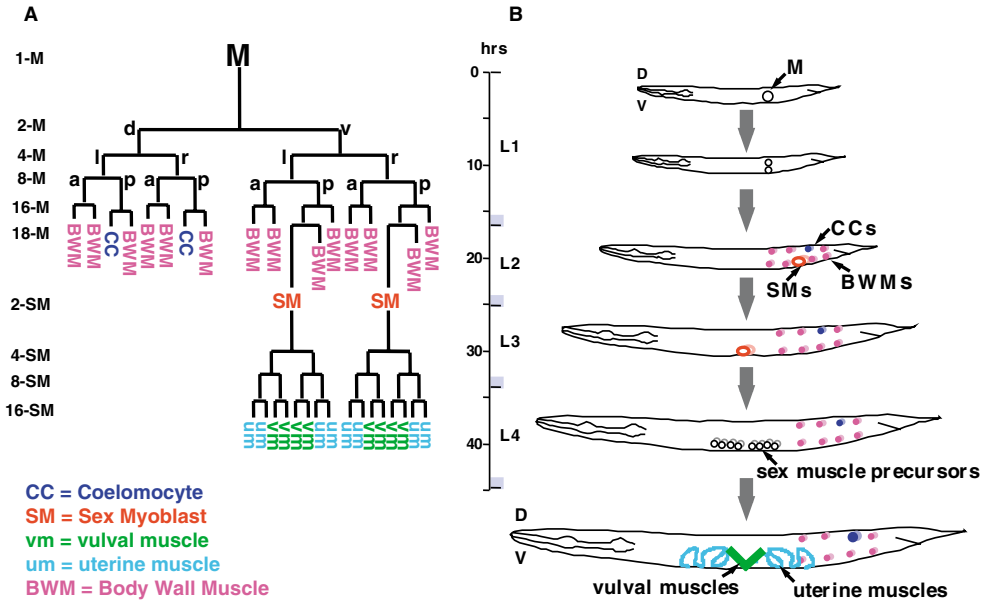

Fig. 1. The *C. elegans* hermaphrodite postembryonic M lineage. Times are indicated post-hatching at 25°C. (**A**) The M lineage showing all differentiated cell types that arise from M [modified from Sulston and Horvitz (Sulston and Horvitz, 1977)]. (**B**) A schematic lateral view of the M lineage through larval development. a, anterior; d, dorsal; l, left; p, posterior; r, right; v, ventral.

MATERIALS AND METHODS

C. elegans strains

Strains were maintained and manipulated using standard conditions (Brenner, 1974). Analyses were performed at 20°C, unless otherwise noted. The following strain was generated to visualize the M lineage in *fozi-1(cc609)* mutant animals throughout postembryonic development: LW0679 [*fozi-1*(*cc609*) *ccIs4438*(*intrinsic CC::gfp*) III; *ayIs2*(*egl-15::gfp*) IV; *ayIs6*(*hlh-8::gfp*) X]. The strain LW0081 [*ccIs4438*(*intrinsic CC::gfp*) III; *ayIs2*(*egl-15::gfp*) IV; *ayIs6*(*hlh-8::gfp*) X] was used in parallel as a wild-type control. The strain LW0064 [*cup-5(ar465) fozi-1(cc609)* III; *jjIs64(arg-1::gfp)* V; *arIs39(secreted CC::gfp)* X] was used to generate transgenic lines for rescue. *Intrinsic CC::gfp* is a twist-derived coelomocyte marker (Harfe et al., 1998b). *Secreted CC::gfp* is another coelomocyte marker using a *myo-3::secreted GFP* construct (Harfe et al., 1998a). Additional M lineage-specific reporters were as described in Kostas and Fire (Kostas and Fire, 2002). The M lineage was followed in live animals under a fluorescence stereomicroscope and confirmed using a compound microscope. Other strains used in this work are:

LG II: *hlh-1(cc561ts), hlh-1(cc450)/mIn1[dpy-10(e128) mIs14]* II (Harfe et al., 1998a)

LG III: *mab-5(e1239)* (Kenyon, 1986), *fozi-1(tm0563)* (gift from Shohei Mitani, Tokyo Women's Medical University School of Medicine, Japan), *ceh-20(n2513)* (Liu and Fire, 2000), WM31: *dpy-17(e164) vab-7(e1562)*

LG V: *him-5(e1467)* (Hodgkin et al., 1979)

LG X: *mls-2(cc615)* (Jiang et al., 2005), *hlh-8(nr2061)* (Corsi et al., 2000)

The CB4856 strain (Hodgkin and Doniach, 1997) was used for snip-SNP mapping of fozi-1.

Mutagenesis screens and analysis of *fozi-1*

In screens for mutants with M lineage defects (Jiang et al., 2005; Foehr et al., 2006), four recessive mutations (*cc607*, *cc608*, *cc609* and *cc610*) were isolated that failed to complement one another. These alleles define the *fozi-1* locus. Mapping and complementation analysis of *fozi-1* was carried out using standard methods by monitoring the number of CCs using the *CC::gfp* markers described above. Three-factor mapping using *dpy-17* and *vab-7* and snip-SNP mapping (Wicks et al., 2001) placed *fozi-1* between cosmids K04H4 and F54G8 on chromosome 3. The molecular lesions of *fozi-1* mutant alleles were identified through sequencing PCR products of genomic fragments spanning the entire coding region of K01B6.1.

Plasmid constructs and transgenic lines

A full-length *fozi-1* cDNA was generated by piecing together two cDNA clones, *yk288g3* and *yk779b02* (gifts from Yuji Kohara, National Institute of Genetics, Japan). A 5 kb fragment spanning the entire coding region and 3′ UTR of *fozi-1* was PCR amplified from N2 genomic DNA using the iProof™ High-Fidelity DNA Polymerase (Bio-Rad). The cDNA and PCR product were used to generate the following constructs:

Forced expression constructs:
pNMA37, *hlh-8p::fozi-1::fozi-1 3′UTR*
pNMA36, *hsp-16p::fozi-1::fozi-1 3′UTR*
Recombinant fusion constructs for protein expression in bacteria:
pNMA04, GST-*fozi-1* cDNA (amino acids 1-171)
pNMA27, GST-*fozi-1* cDNA (full length)
pNMA28, GST-*fozi-1* cDNA (amino acids 366-732)
pGEX-6P-3-*cyk-1* cDNA (amino acids 681-1435 of *cyk-1*)

All constructs were confirmed by sequencing. Details on all constructs are available upon request. Transgenic lines were generated using the plasmid pRF4 (Mello et al., 1991) as a marker.

RNAi

Plasmids *yk288g3* and *yk779b02* were used as templates for synthesizing dsRNA against *fozi-1* as described by Fire and colleagues (Fire et al., 1998). Plasmid *yk116b7* was used for synthesizing dsRNA against M01A8.2. All yk clones are from Yuji Kohara (National Institute of Genetics, Japan). dsRNAs for *hlh-1*, *mab-5* and *ceh-20* were synthesized using plasmids pVZ1200 (gift from Mike Krause, NIDDK, NIH, USA), pJKL718.2 and pJKL422.1 (Liu and Fire, 2000), respectively. *fozi-1*, *M01A8.2* or *ceh-20* dsRNA was injected into gravid adults of our wild-type reference strain LW0081. Progeny from the injected animals were scored for M lineage phenotypes and, in the case of *ceh-20*, for FOZI-1 expression via immunostaining.

For *hlh-1(RNAi)* and *mab-5(RNAi)*, synchronized L1 animals expressing various M lineage GFP markers were soaked in *hlh-1* dsRNA, *mab-5* dsRNA, or both, for 24-48 hours following the protocol of Maeda and colleagues (Maeda et al., 2001). Animals were allowed to recover at 20°C and scored for M lineage phenotypes. Water was used as a soaking control.

Heat-shock experiments

The following strains were generated and used in the heat-shock experiments:

Table 1. M lineage defects of *fozi-1* mutant alleles

Genotype	Number of M-derived CCs (*intrinsic CC::gfp*)	Number of M-derived BWMs (*myo-3::gfp*)	Number of SM-like cells (*hlh-8::gfp*)	Number of vm1-like cells (*egl-15::gfp*)
Wild type	2 (*n*>100)	14 (*n*=5)	2 (*n*>100)	4 (*n*>100)
cc607	0 (*n*>100)	nd	4.11±0.88 (*n*=55)	8.26±1.39 (*n*=31)
cc608	0 (*n*>100)	nd	nd	nd
cc609	0 (*n*>100)	12.5±0.85 (*n*=10)	4.10±0.86 (*n*=58)	8.41±1.54 (*n*=37)
cc610	0.58±0.78 (*n*=161)†	nd	3.17±0.97 (*n*=88)	6.45±1.41 (*n*=64)
tm0563	0 (*n*>100)	nd	4.01±0.85 (*n*=61)	8.81±1.37 (*n*=42)

Data indicated are average counts plus or minus standard deviation where applicable.
†60% of animals scored had 0 M-derived CCs, 21% had 1 and 19% had 2. CCs, coelomocytes; BWM, body wall muscles; SM, sex myoblasts; nd, not determined.

ccIs4251(myo-3::gfp); jjEx[hsp::hlh-1(pPD50.63) + rol-6(d)]
ccIs4251(myo-3::gfp); jjEx[hsp::fozi-1(pNMA36) + rol-6(d)]
ccIs4438(intrinsic CC::gfp); ayIs2(egl-15::gfp); ayIs6(hlh-8::gfp); jjEx[hsp::hlh-1 + rol-6(d)]
ccIs4438(intrinsic CC::gfp); ayIs2(egl-15::gfp); ayIs6(hlh-8::gfp); jjEx[hsp::fozi-1 + rol-6(d)]
ccIs4438(intrinsic CC::gfp); ayIs2(egl-15::gfp); ayIs6(hlh-8::gfp); jjEx[hsp::hlh-1 + hsp::fozi-1 + rol-6(d)]

Two different heat-shock protocols were used to test the myogenic potential of FOZI-1. In each case, global ectopic expression of FOZI-1 was confirmed by anti-FOZI-1 antibody staining 4 hours after heat shock. The first protocol was the same as described in Fukushige and Krause (Fukushige and Krause, 2005). One- to two-cell embryos were harvested and incubated at 20°C for 30 minutes. Embryos were then heat shocked for 30 minutes at 37°C and allowed to recover at 20°C. Embryos were observed periodically over a 20 hour window for ectopic *myo-3::gfp* expression and an arrested development phenotype. For the second protocol, transgenic animals were given multiple heat-shock pulses (five to seven pulses) starting from mid-embryo to early L1 stage through to adulthood. Heat-shock pulses were performed for 30 minutes at 37°C followed by 3 to 4 hours at 20°C before subsequent heat-shock treatments. Heat-shocked animals were scored for their M lineage phenotypes. In both experiments, heat-shocked non-transgenic animals were used as negative controls.

In vitro actin-binding assays

Plasmids pNMA27, pNMA28 and pGEX-6P-3-*cyk-1*^{FH1FH2COOH} were used to generate GST-fusion proteins in BL21(DE3) cells for FOZI-1, FOZI-1 FH2 domain and CYK-1 FH1FH2 domains plus COOH-terminal residues, respectively. All GST-fusion proteins were bound to glutathione sepharose 4B beads (Amersham Biosciences) and cleaved from GST by GST-3CPro precision protease (Amersham Biosciences) and soluble FOZI-1, FOZI-1^{FH2}, or CYK-1^{FH1FH2COOH} were extracted. GST-Bni1p^{FH1FH2COOH} was purified as previously described (Pruyne et al., 2002). Samples were analyzed by SDS-PAGE.

The effects of FOZI-1 on rates of actin polymerization and barbed end capping of actin filaments were examined using pyrene-actin assays (Pollard, 1983) with the above-purified recombinant proteins. Recombinant FOZI-1 proteins were incubated with F-actin in co-sedimentation assays to test whether FOZI-1 binds filamentous actin (Bretscher, 1981). Details on all actin-based assays are available upon request.

Antibody production and immunofluorescence staining

The N-terminus of FOZI-1 (amino acids 1-171) was cloned into pGEX-4T-1 (Smith and Johnson, 1988). The resulting plasmid pNMA04 was transformed into BL21(DE3)pLysS cells. Fusion proteins were purified from glutathione sepharose 4B beads (Amersham Biosciences) and further purified by SDS-PAGE. Gel slices containing purified FOZI-1 protein were used to immunize guinea pigs (Cocalico Biologicals, PA). Resulting antiserum was tested by western blot analysis using bacterially expressed GST-FOZI-1 fusion proteins. Antibodies were affinity purified against GST-FOZI-1 bound to a nitrocellulose membrane (Olmsted, 1981; Smith and Fisher, 1984).

Animal fixation and immunostaining were performed following the protocol of Hurd and Kemphues (Hurd and Kemphues, 2003). For immunostaining with HLH-1 antibodies, animals were fixed and stained following the protocol of Harfe and colleagues (Harfe et al., 1998a). The following antibodies were used: affinity purified anti-FOZI-1 (CUMC-GP19; 1:50), goat anti-GFP (Rockland Immunochemicals; 1:5000), rat anti-MLS-2 (Jiang et al., 2005) (1:600) and rabbit anti-HLH-1 (Harfe et al., 1998a) (1:400). All secondary antibodies were from Jackson ImmunoResearch Laboratories and used in a dilution of 1:100 to 1:200. Differential interference contrast and epifluorescence microscopy were performed using a Leica DMRA2 compound microscope. Images were captured with a Hamamatsu Orca-ER Camera using the Openlab software (Improvision). Subsequent image analysis was performed using Adobe Photoshop 7.0 and Adobe Illustrator CS.

RESULTS

fozi-1 mutants display cell fate specification defects in the M lineage

In screens to identify mutants affecting M lineage development (see Materials and methods), we isolated four recessive mutations that failed to complement one another: *cc607*, *cc608*, *cc609* and *cc610*. These mutations defined the *fozi-1* locus (see below). Animals homozygous for these mutations lacked M-derived CCs, with 100% penetrance in *cc607*, *cc608* and *cc609* and 81% penetrance in *cc610* (Table 1, Fig. 2).

To determine the basis for the missing CCs in these mutants, we followed the M lineage in *cc609* mutant animals using a combination of cell-type-specific markers. Using the *hlh-8::gfp* reporter as a marker for undifferentiated cells of the M lineage (Harfe et al., 1998b), we found that the M mesoblast in *cc609* mutant animals gave rise to a total of 18 descendants (Fig. 2J-L, data not shown), like wild type (Fig. 2I). However, the fates of these 18 cells in *cc609* mutants were not specified correctly. Of the 18 cells that arose from M in wild-type animals, 14 became BWMs, two became CCs and two became SMs (Fig. 1). In *cc609* mutants, however, both M-derived CCs (visualized using the *intrinsic cc::gfp* marker) (Harfe et al., 1998b) were missing, fewer than 14 M-derived BWMs (visualized using *myo-3::gfp*) (Fire et al., 1998) were present (Table 1, Fig. 2J-L), and more than two of the 18 M-derived cells displayed SM-like characteristics (*hlh-8::gfp* expression, SM shape, enlarged size and potential to migrate to the presumptive vulval region) (Table 1, Fig. 2A-D). Two of the SM-like cells in *cc609* mutants always migrated to the ventral side near the presumptive vulval region and generated the correct number of sex muscles that attached properly, as visualized by *egl-15::gfp*, *arg-1::gfp*, *myo-3::gfp* and polarized light microscopy. The remaining SM-like cells divided one to three times and gave rise to extra sex muscles either around the vulva or in the posterior region of the animal (Table 1, Fig. 2G-H, data not shown). Thus *cc609* mutants exhibit cell fate transformations from M-derived CCs and BWMs to SMs (Fig. 2J-L). Similar M lineage defects were also observed in *cc607*, *cc608* and *cc610* mutant animals (Table 1).

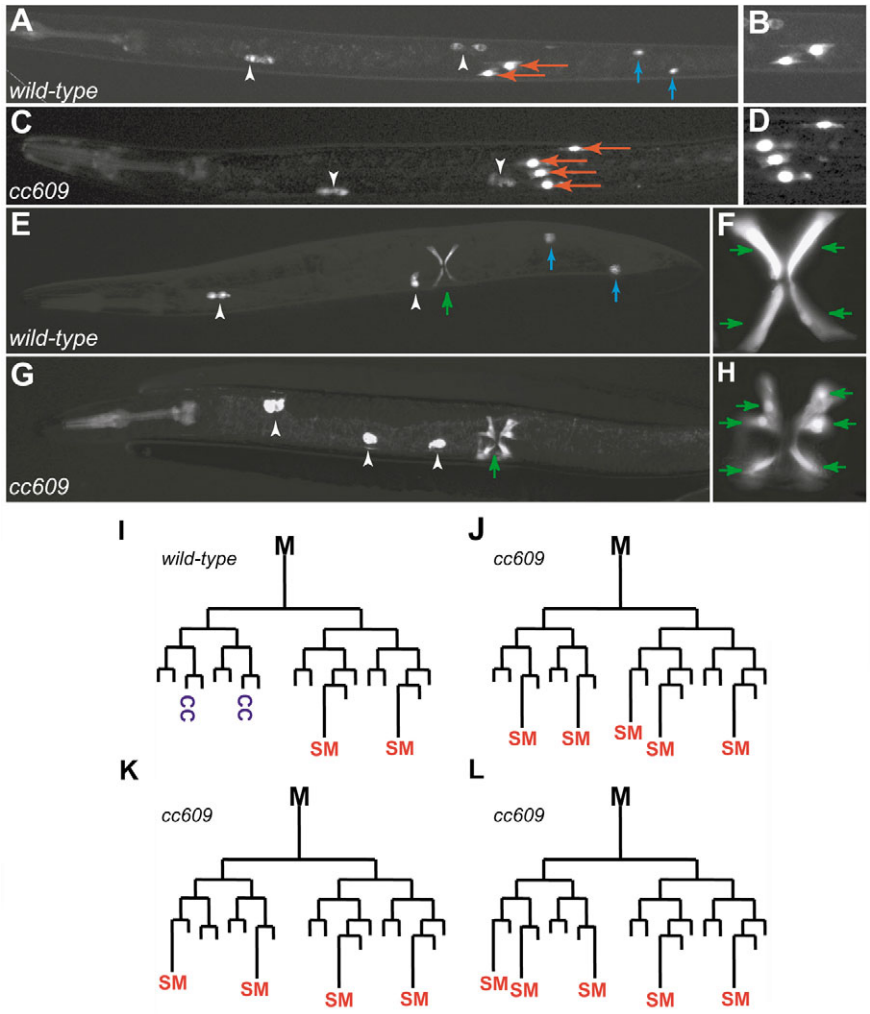

Fig. 2. The M lineage phenotypes of *cc609* mutants. All images are ventral/lateral views with anterior to the left. (**A-H**) Wild-type (A,B,E,F) and *cc609* mutant (C,D,G,H) animals at the late L2 stage (A-D) and adult stage (E-H). SMs are visualized using *hlh-8::gfp* and labeled with red arrows. CCs are visualized using *intrinsic CC::gfp*; embryonic CCs are labeled with white arrowheads and M-derived CCs with blue arrows. Type I vulval muscles are visualized using *egl-15::gfp* and labeled with green arrows. Note the presence of two SMs in the wild-type larva (A,B) and four SM-like cells in the *cc609* larva (C,D). B and D show the SM-like cells at higher magnification. Also note the lack of M-derived CCs in *cc609* larva (C,G) compared with wild-type animals (A,E). *cc609* adults have extra type I vulval muscles (vm1-like cells) (G,H) compared with wild type (E,F). F and H show the vulval muscles in higher magnification. (**I-L**) Representations of the hermaphrodite M lineage in wild-type (I) and different *cc609* mutant (J-L) animals. Unmarked cells refer to BWMs. (I) Wild-type animals always give rise to two CCs, two SMs and 14 BWMs. (J-L) *cc609* mutant animals consistently have a loss of M-derived CCs and some BWMs, with the concomitant gain of SM-like cells.

fozi-1 encodes a novel formin with two C_2H_2 Zn fingers and an FH2 formin homology domain

We mapped *cc609* to an interval between cosmids K04H4 and F54G8 in the middle of chromosome 3. Two overlapping cosmids in this region, M01A8 and K01B6, rescued the M lineage defects of *cc609* mutants. We performed RNAi for each of the two genes located at the junction between M01A8 and K01B6, M01A8.2 and K01B6.1 (see Materials and methods). RNAi of M01A8.2 gave no M lineage defects. However, RNAi of K01B6.1 in wild-type animals resulted in similar M lineage defects to those seen in *cc609* mutant animals. Sequencing the coding regions of K01B6.1 in *cc607*, *cc608*, *cc609* and *cc610* mutant animals showed that they all contained molecular lesions in the K01B6.1 coding region (Fig. 3A). *cc607* and *cc608* contained the same nonsense mutation at residue 112 (CAG to TAG, Gln to amber stop). The *cc609* mutant contained a deletion that spanned residues 160 to 260 of K01B6.1 and caused a frameshift in the remaining coding sequence (Fig. 3A). In *cc610* mutants, there was a missense mutation at residue 207 (CGA to TGA, Pro to Leu) (Fig. 3A). During the course of our studies, the National Bioresource Project for the Experimental Animal Nematode *C. elegans* generated another deletion allele of K01B6.1, *tm0563*, which deletes a larger region than *cc609* and also results in a frameshift (Fig. 3A). *tm0563* mutant animals displayed similar M lineage phenotypes to *cc609* animals (Table 1). As *cc607*, *cc608*, *cc609* and *tm0563* all exhibited 100% penetrance in their M lineage defects (Table 1), and they contained either early termination codons or deletions in K01B6.1 (Fig. 3A), all four alleles are probably null alleles. Additional evidence supporting this is provided by the immunostaining results discussed below.

The predicted protein encoded by K01B6.1 is FOZI-1, a 732-amino acid protein with three distinct motifs (Fig. 3B): a glutamine-rich region (residues 88-133), two C_2H_2 zinc finger motifs (residues 177-201) and an FH2 formin homology domain (residues 369-732). The glutamine-rich region and the zinc finger motifs are characteristics of transcription factors (Matsuzaki et al., 1995; Iuchi, 2001; Stepchenko and Nirenberg, 2004). The FH2 domain is conserved among a large family of proteins called formins, which are present in a range of organisms, from yeast to humans (Higgs and Peterson, 2005). Formins have been shown to use their FH2 domains to form dimers that bind actin and play crucial roles in multiple processes of actin dynamics, such as nucleation, capping, severing and bundling of actin filaments (Pruyne et al., 2002; Sagot et al., 2002; Kovar et al., 2003; Zigmond et al., 2003; Harris et al., 2004; Xu et al., 2004; Michelot et al., 2005; Moseley and Goode, 2005). The FH2 domain of FOZI-1 is unique in that it contains many of the conserved residues involved in dimerization, but lacks the key residues crucial for actin binding (see Fig. S1A in the supplementary material). We tested whether the FH2 domain of FOZI-1 or the full-length FOZI-1 protein could bind filamentous actin, induce actin polymerization or cap the barbed-ends of actin filaments in vitro. We found that FOZI-1 was unable to polymerize actin filaments, while the *C. elegans* CYK-1 FH1FH2 protein domains were fully active in

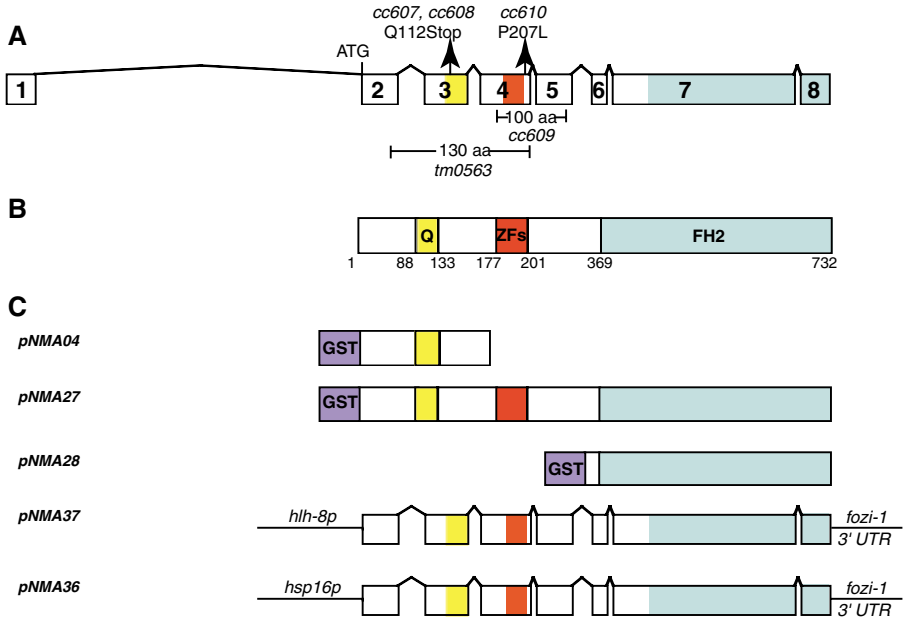

Fig. 3. *fozi-1* encodes a novel protein. (**A**) *fozi-1* gene structure (not drawn to scale) showing molecular lesions of *fozi-1* mutants. The first intron of *fozi-1* spans 7 kb upstream of the translation start site. (**B**) The structural motifs of FOZI-1 include a Q-rich region (amino acids 88-133), two C_2H_2 zinc finger motifs (amino acids 177-201) and an FH2 formin homology domain (amino acids 369-732). (**C**) pNMA04, pNMA27 and pNMA28 are *fozi-1* fusion constructs used to purify recombinant FOZI-1 fragments. pNMA36 and pNMA37 were used in transgenic assays.

this process (see Fig. S1B in the supplementary material). Furthermore, FOZI-1 was unable to bind actin or show capping activity in vitro (data not shown). As residues crucial for dimerization in the FH2 domain of FOZI-1 are conserved, the FOZI-1 FH2 domain probably functions as a dimerization domain, consistent with in vitro data obtained by Johnston and colleagues (Johnston et al., 2006).

FOZI-1 is a nuclear protein expressed in the M-derived CC and BWM precursors

As described above, *fozi-1* mutant animals exhibited cell fate transformations from M-derived CCs and BWMs to SMs. To begin to understand how FOZI-1 functions in regulating fate specification in the M lineage, we examined the expression pattern of FOZI-1 during development. We generated antibodies to FOZI-1 and performed immunostaining to detect the endogenous FOZI-1 protein (see Materials and methods). The antibodies specifically recognized a protein of the predicted size for FOZI-1 (~80 kD) on western blots using worm extracts (data not shown), and failed to detect any signal in *cc609* mutant embryos and larvae (Fig. 4C,D,T).

Using these antibodies, we found that FOZI-1 protein was localized in nuclei of a distinct set of cells in wild-type animals. Expression of FOZI-1 was first detectable in a small subset of nuclei (probably neuroblasts) in embryos at the 2-fold stage (Fig. 4A-B). During larval development, FOZI-1 expression was restricted to a subset of unidentified neurons in the head (seven to 12 cells) and along the ventral nerve cord (five to seven cells) (Fig. 4E-F). FOZI-1 was also present transiently during the L1 larval stage in cells derived from the M lineage (see below).

To examine the M lineage expression pattern of FOZI-1, we performed double-labeling experiments using anti-FOZI-1 antibodies and the M lineage-specific *hlh-8::gfp* marker (Harfe et al., 1998b). FOZI-1 expression in the M lineage was first detectable in the nuclei of M.d and M.v at the 2-M stage (in 43% of the animals stained, n=21, Fig. 4G-I). This expression persisted through the next three rounds of cell divisions, such that all animals (n>50) at the 4-M through to the 16-M stage showed FOZI-1 expression in the M lineage (Fig. 4J-L). At the 16-M stage, two cells on the ventral side (M.vlpa and M.vrpa) divide one more time to produce two SMs and two BWM precursors and reach the 18-M stage (Fig. 1) (Sulston and Horvitz, 1977). At the 18-M stage, FOZI-1 was still detectable in the undifferentiated BWMs and CCs, but not in the SMs (n=22; Fig. 4M-O). This expression of FOZI-1 at the 18-M stage appeared transiently and quickly became undetectable in the differentiated BWMs and CCs. FOZI-1 expression was not detected in the SM lineage (n>50; Fig. 4P-R, data not shown). The expression pattern of FOZI-1 in the M lineage is summarized in Fig. 4S. Thus, expression of FOZI-1 is tightly regulated within the M lineage at the time when BWM and CC cell fate specification occurs.

Residues proximal to the C_2H_2 zinc fingers are required for FOZI-1 function in the M lineage

To determine whether FOZI-1 expression and subcellular localization were lost in *fozi-1* mutants, we performed FOZI-1 staining in all of the *fozi-1* mutants at all developmental stages. As discussed above, *cc609* animals had no detectable levels of FOZI-1 at any stage during development (Fig. 4C,D,T). *cc607* and *tm0563* also showed no FOZI-1 immunostaining at any stage (data not shown; we did not examine *cc608* animals, because *cc607* and *cc608* contain the same molecular lesion). These results are consistent with our hypothesis that *cc607*, *cc609* and *tm0563* are null alleles. Animals mutant for *cc610*, however, showed nuclear anti-FOZI-1 staining in a pattern identical to wild-type animals in the head neurons, ventral nerve cord and the M lineage (Fig. 4U; n>50). As *cc610* mutants exhibited M lineage defects (Table 1) and the missense mutation in *cc610* is located six residues downstream of the second histidine residue of the second zinc finger (Fig. 3A), we conclude that the residues surrounding the C_2H_2 zinc fingers are required for proper FOZI-1 function in the M lineage.

FOZI-1 functions within the M lineage for proper CC and BWM cell fate specification

The expression pattern of *fozi-1* and the M lineage defects of *fozi-1* mutants suggest that FOZI-1 functions within the M lineage to specify the fates of the CCs and BWMs. To directly test this hypothesis, we expressed *fozi-1* specifically in the M lineage in *cc609* mutants using the *hlh-8* promoter (Harfe et al., 1998b). Transgenic

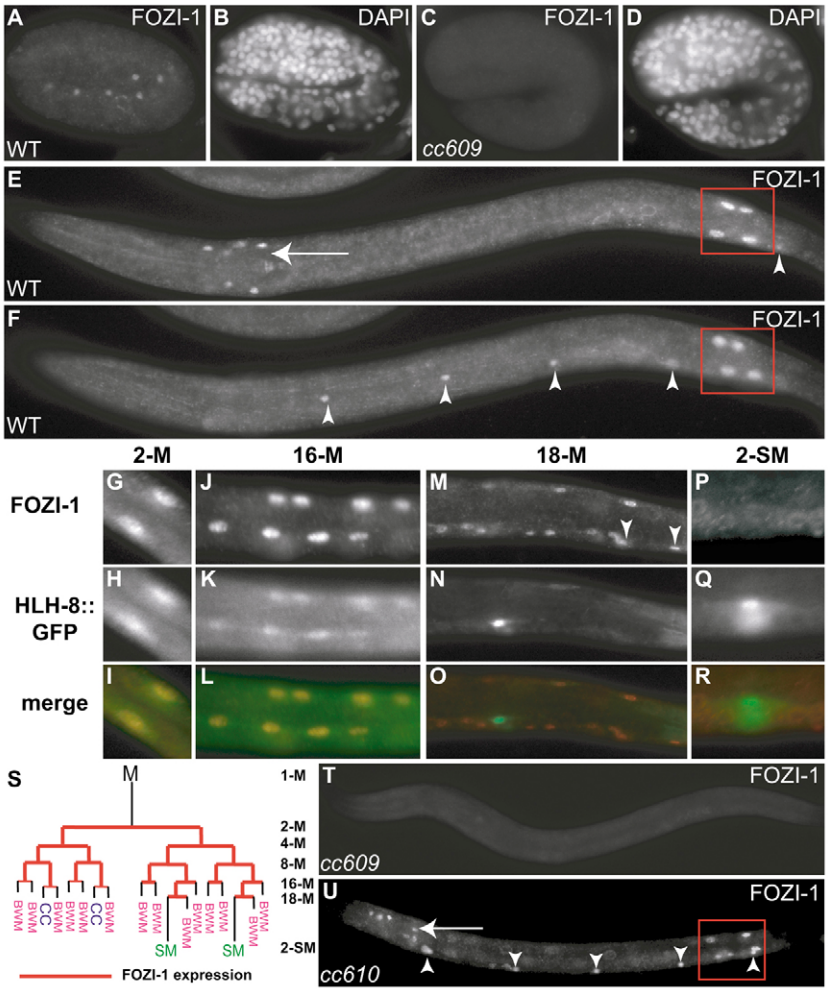

Fig. 4. Expression pattern of FOZI-1 in wild-type, *cc609* and *cc610* hermaphrodites and embryos. All images are lateral views with anterior to the left and dorsal up (unless otherwise noted). (**A-D**) Wild-type (A,B) and *cc609* (C,D) embryos stained with anti-FOZI-1 antibody (A,C) and DAPI (B,D). Nuclear FOZI-1 is seen in a subset of cells at the 2-fold stage of embryogenesis in wild-type (A) but not in *cc609* (C) embryos. (**E**,**F**) FOZI-1 staining in a wild-type L1 larva on two different focal planes. FOZI-1 was observed in the nuclei of 7-12 head neurons (arrow, E) and 5-7 cells along the ventral nerve cord (arrowheads, E,F) and in cells derived from the M lineage (red box, E,F). (**G-R**) Double labeling with anti-FOZI-1 antibody and *hlh-8::gfp* at the 2-M (G-I), 16-M (J-L), 18-M (M-O) and 2-SM (P-R) stages in wild-type animals. Anti-FOZI-1 antibody staining is shown in panels G,J,M,P; *hlh-8::gfp* is shown in panels H, K,N,Q; the corresponding merged images are shown in panels I,L,O,R. FOZI-1 staining was first detected at the 2-M stage (G-I) and persisted through the 16-M (J-L) stages. At the 18-M stage (M-O) FOZI-1 is still present in all undifferentiated CC and BWM precursors but is absent in the SMs. Arrowheads in panel M denote cells in the ventral nerve cord. (P-R) FOZI-1 is not present in the 2-SM cells and the subsequent SM lineage (data not shown). (**S**) Summary of FOZI-1 expression in the M lineage. The wild-type M lineage is shown with overlay of FOZI-1 expression highlighted in red. (**T**,**U**) Staining of *cc609* (T) and *cc610* (U) animals at mid-L1 stage using anti-FOZI-1 antibodies. (T) No FOZI-1 was detected in *cc609* animals. (U) Wild-type level and localization pattern of FOZI-1 are detected in *cc610* mutant animals in head neurons (arrow), ventral nerve cord (arrowheads) and the M lineage (red box).

animals carrying an *hlh-8p::fozi-1* transgene (Fig. 3C) in the *cc609* mutant background showed M lineage-specific expression of *fozi-1* (data not shown). This M lineage-specific expression was sufficient to restore M-derived CCs in *cc609* mutant animals (23.2%, *n*=56). The low level of rescue may be attributed to the difference between endogenous *hlh-8* and *fozi-1* expression patterns: *fozi-1* persists slightly longer than *hlh-8* in the BWM and CC precursors (Harfe et al., 1998b) (Fig. 4M-O). Thus, FOZI-1 appears to function cell autonomously within the M lineage for proper mesodermal cell fate specification.

FOZI-1 functions redundantly with CeMyoD (HLH-1) to specify BWM fates in the M lineage

Previous studies (Harfe et al., 1998a) have shown that the *C. elegans* MyoD ortholog, Ce-MyoD (HLH-1), is expressed in the M lineage in a pattern like that of FOZI-1 (except that HLH-1 persists in all differentiated M-derived BWMs, whereas FOZI-1 does not) and that *hlh-1* mutants showed similar CC and BWM to SM fate transformation as *fozi-1* mutants. To examine the functional relationship between FOZI-1 and HLH-1, we examined the expression and nuclear localization of HLH-1 in *fozi-1(cc609)* mutants and of FOZI-1 in the temperature-sensitive *hlh-1(cc561ts)* mutants at the non-permissive temperature (25°C). As shown in Fig. 5A-D, expression and nuclear localization of FOZI-1 in *hlh-1(cc561ts)* and HLH-1 in *fozi-1(cc609)* were normal. Thus, HLH-1 and FOZI-1 do not regulate the expression or subcellular distribution of each other.

As both *hlh-1* and *fozi-1* mutant animals exhibit loss of some, but not all, BWMs derived from the M lineage (Harfe et al., 1998a) (this work), we investigated the possibility that *hlh-1* and *fozi-1* act redundantly. Because *hlh-1* null mutants are embryonic/L1 lethal due to the essential functions of HLH-1 in proper differentiation of the embryonically derived BWMs (Chen et al., 1992; Chen et al., 1994), we used two approaches to assess the possible redundancy of HLH-1 and FOZI-1 in the M lineage. We first soaked *fozi-1(cc609)* L1 larvae with *hlh-1* dsRNA to deplete levels of HLH-1 in *fozi-1(cc609)* worms [referred to as *hlh-1(RNAi); fozi-1(cc609)*; see Materials and methods]. We also generated *hlh-1(cc561ts); fozi-1(cc609)* double mutants and examined them at the restrictive temperature (25°C) for *cc561ts*. Both approaches gave almost identical results. The *hlh-1(cc561ts); fozi-1(cc609)* or *hlh-1(RNAi); fozi-1(cc609)* animals had a significant increase in the number of SM-like cells (Fig. 6A) and a concomitant decrease in the number of M-derived BWMs (Fig. 6B) when compared with *fozi-1(cc609)*, *hlh-1(cc561ts)* or *hlh-1(RNAi)* single mutants. The increased number of SM-like cells in *hlh-1(cc609ts); fozi-1(cc609)* or *hlh-1(RNAi); fozi-1(cc609)* animals was correlated with the significantly higher number of type I vulval-muscle-like cells (vm1-like cells) that express *egl-15::gfp* (data not shown). To distinguish whether these changes in the numbers of SMs and BWMs arose from cell fate transformations or cell proliferation defects, we followed the M lineage closely in three *hlh-1(RNAi); fozi-1(cc609)* mutant animals using a combination of *hlh-8::gfp* and DIC optics. We did not observe any proliferation defects in the first four rounds of cell

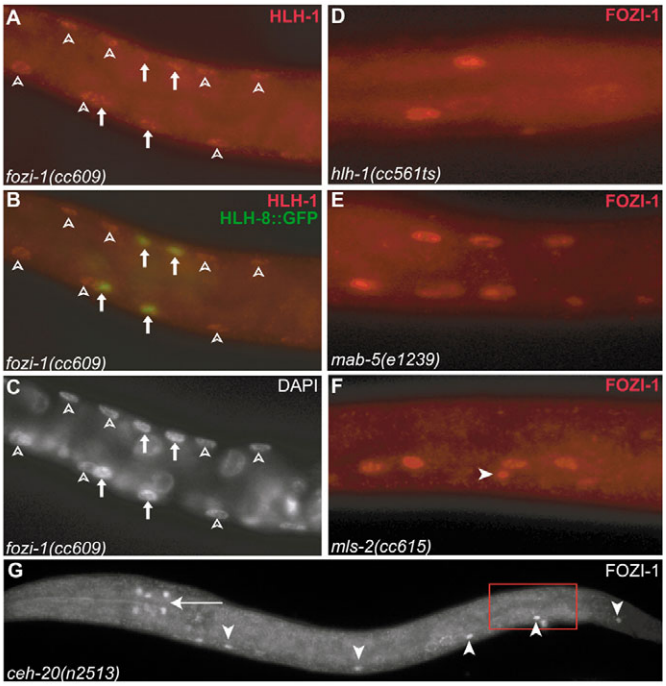

Fig. 5. Expression of FOZI-1 in different M lineage mutants. (**A-C**) A *fozi-1(cc609); ayIs6(hlh-8::gfp)* mutant animal at the 8-M stage stained with anti-HLH-1 antibody (red in A,B) and DAPI (C). White arrows represent M lineage as marked by *hlh-8::gfp*. Embryonically derived BWMs are denoted by open arrowheads. (**D-F**) Anti-FOZI-1 staining in *hlh-1(cc561ts)* (D), *mab-5(e1239)* (E) and *mls-2(cc615)* (F) animals. FOZI-1 is present in the M lineage of all three mutants. Arrowhead denotes a cell from the ventral nerve cord (F). (**G**) A *ceh-20(n2513)* animal stained with anti-FOZI-1 antibody. FOZI-1 is detected in the head neurons (arrow) and the ventral nerve cord (arrowheads), but not in the M lineage (red box).

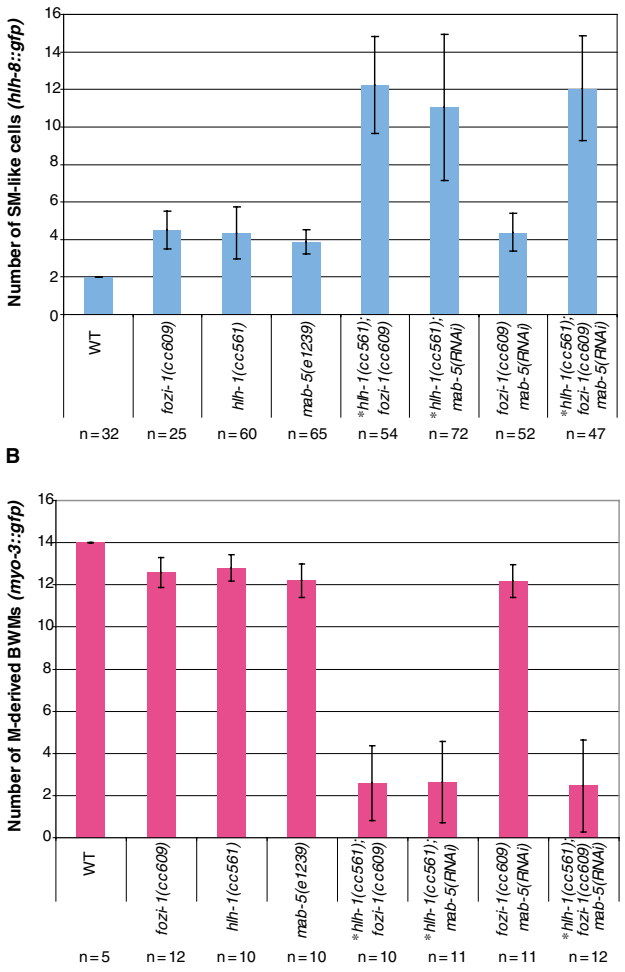

Fig. 6. HLH-1 functions redundantly with FOZI-1 and MAB-5 to specify M-derived BWMs. (**A**,**B**) Quantification of the number of SM-like cells (expressing *hlh-8::gfp*) (A) and M-derived BWMs (expressing *myo-3::gfp*) (B). *n* values are given for each genotype scored. Mean values are shown with error bars representing standard deviation for each sample set. All animals showed normal proliferation in the early M lineage up to the 16-M stage. The number of SM-like cells and M-derived BWMs were also scored in the following animals: *mab-5(RNAi)*, *hlh-1(RNAi)*, *hlh-1(RNAi); mab-5(e1239)*, *hlh-1(RNAi); fozi-1(cc609)*, *hlh-1(RNAi); fozi-1(cc609) mab-5(RNAi)* and *hlh-1(cc561ts+RNAi); fozi-1(cc609) mab-5(e1239)*. For each genotype, more than 50 animals were scored for the number of SMs and more than ten animals were scored for the number of M-derived BWMs. *A small percentage of these animals lacked all M-derived BWMs and had a total of 16-18 SM-like cells.

divisions of the M mesoblast in these animals. Instead, all three animals exhibited a fate transformation from M-derived BWMs and CCs to SMs. There were eight SM-like cells and one M-derived BWM on the right side of animal #1, and nine SM-like cells and 0 M-derived BWMs on the right side of animal #2. Animal #3 was monitored on both the right and the left sides. There were a total of 12 SM-like cells and four M-derived BWMs in this animal. All three animals had the correct number of embryonically derived BWMs (data not shown). These observations indicate that FOZI-1 and HLH-1 function redundantly to specify striated BWM fate in the postembryonic mesoderm.

FOZI-1 functions in the same process as the Hox factor MAB-5 in specifying M-derived BWMs

In addition to HLH-1 and FOZI-1, mutations in the Hox gene *mab-5* also result in the fate transformation of both M-derived CCs and some, but not all, M-derived BWMs to SMs (Harfe et al., 1998b) (Fig. 6A,B). We therefore examined the relationship among MAB-5, FOZI-1 and HLH-1 in M-derived BWM fate specification. Because *mab-5* and *fozi-1* map very close to each other on chromosome 3, we used RNAi to knock down the expression of *mab-5* in *hlh-1(cc561ts)*, *fozi-1(cc609)* or *hlh-1(cc561ts); fozi-1(cc609)* mutants (see Materials and methods). We first established that *mab-5(RNAi)* caused similar M lineage phenotypes to the null *mab-5(e1239)* mutant (Fig. 6, data not shown). We then followed the M lineage and counted the number of M-derived BWMs and SMs in various mutants soaked with *mab-5* dsRNA. All mutant animals exhibited normal proliferation in the early M lineage (data not shown). However, their terminal M lineage phenotypes differed from each other. As shown in Fig. 6A,B, *fozi-1(cc609) mab-5(RNAi)* animals behaved just like *fozi-1(cc609)* or *mab-5(RNAi)* single mutant animals with only a few M-derived BWMs transformed to SMs, whereas *hlh-1(cc561ts); mab-5(RNAi)* animals behaved just like *hlh-1(cc561ts); fozi-1(cc609)* animals in that most, if not all, M-derived BWMs were transformed to SMs (Fig. 6A,B). *hlh-1(cc561ts); fozi-1(cc609) mab-5(RNAi)* animals were indistinguishable from *hlh-1(cc561ts); fozi-1(cc609)* animals or *hlh-1(cc561ts); mab-5(RNAi)* animals in their BWM or SM phenotype (Fig. 6A,B). Collectively, these results suggest that both MAB-5 and

FOZI-1 function redundantly with HLH-1 to properly specify striated BWM fates in the M lineage and that MAB-5 and FOZI-1 act in the same process.

mab-5 is expressed in the M mesoblast, and its expression persists throughout the M lineage (S. J. Salser, PhD thesis, University of California, 1995). As *mab-5* expression precedes *fozi-1* expression in the M lineage, we asked if *mab-5* is required for *fozi-1* expression. We stained *mab-5(e1239)* null mutant animals with anti-FOZI-1 antibodies and found a wild-type FOZI-1 expression and subcellular localization pattern (Fig. 5E), indicating that *mab-5* is not required for the proper expression and localization of FOZI-1. It is unlikely that *fozi-1* is required for *mab-5* expression, as *fozi-1(cc609)* mutants do not display cleavage orientation defects or loss of *hlh-8* expression in the M lineage (Fig. 2, data not shown), phenotypes exhibited by *mab-5(e1239)* single mutants (Harfe et al., 1998b). Thus, FOZI-1 and MAB-5 do not regulate the expression of each other in the M lineage.

The homeodomain protein CEH-20 is required for *fozi-1* expression in the M lineage

In addition to MAB-5, three other transcription factors crucial for proper M lineage development, CEH-20, MLS-2 and HLH-8, are expressed in the M lineage beginning at the 1-M (or the M mesoblast) stage (Harfe et al., 1998b; Yang et al., 2005; Jiang et al., 2005). We asked whether these factors are required for *fozi-1* expression in the M lineage. We stained animals mutant for the presumed null alleles *mls-2(cc615)* and *hlh-8(nr2061)* using anti-FOZI-1 antibodies and found that *fozi-1* expression level and pattern were not altered (Fig. 5F, data not shown). Similarly, expression of *mls-2* and *hlh-8* in the M lineage does not depend on FOZI-1 (data not shown).

By contrast, when we stained animals from the strong loss-of-function allele *ceh-20(n2513)*, we found that close to 90% of the animals (n=205) lacked *fozi-1* expression in the M lineage (Fig. 5G). M lineage expression of *fozi-1* was also lost in progeny of animals injected with *ceh-20* dsRNA (data not shown). In both *ceh-20(n2513)* and *ceh-20(RNAi)* animals, *fozi-1* expression was still detectable in the head neurons and the ventral nerve cord (Fig. 5G, data not shown), indicating that CEH-20 is specifically required for M lineage expression of *fozi-1*.

DISCUSSION

We have identified a gene, *fozi-1*, encoding a unique zinc finger-FH2 domain-containing protein that is required for proper fate specification in the *C. elegans* postembryonic mesoderm. We have shown that the FH2 domain of the FOZI-1 protein does not bind actin (see Fig. S1 in the supplementary material) and that FOZI-1 is localized to the nucleus (Fig. 4). As FOZI-1 contains a Q-rich region and two C_2H_2 zinc finger motifs that are characteristic of transcription factors (Matsuzaki et al., 1995; Iuchi, 2001; Stepchenko and Nirenberg, 2004), we propose that FOZI-1 acts as a transcription factor required for proper fate specification in the M lineage.

In animals lacking FOZI-1, some M lineage-derived BWMs and non-muscle CCs are transformed to SM-like cells (Fig. 2). As M lineage-specific expression of *fozi-1* rescued these M lineage defects of *fozi-1(cc609)* mutants, we conclude that FOZI-1 functions cell autonomously within the M lineage to specify both BWM and CC fates. FOZI-1 is present in the early M lineage as well as in all M-derived BWM and CC precursors, but not SMs (Fig. 5). It is not clear at present whether FOZI-1 functions early in the M lineage in the multipotent precursors or in the early cell cycle of the terminal BWM, CC or SM cells.

FOZI-1 and CeMyoD function redundantly to specify the striated BWM fate in the M lineage

The stochastic loss of a fraction of M-derived BWMs in *fozi-1(cc609)* mutants is very similar to phenotypes exhibited by animals lacking HLH-1 in the M lineage (Harfe et al., 1998a). We have shown that *hlh-1(cc561ts); fozi-1(cc609)* and *hlh-1(RNAi); fozi-1(cc609)* animals exhibit normal proliferation in the early M lineage, yet most, if not all, of their M-derived BWMs are transformed to SM-like cells. These results demonstrate that FOZI-1 and HLH-1 function redundantly to specify M-derived BWM fates. Although the presence of a few M-derived BWMs in some *hlh-1(cc561ts); fozi-1(cc609)* or *hlh-1(RNAi); fozi-1(cc609)* animals could be due to the partial loss-of-function nature of the *hlh-1(cc561ts)* mutation or the inefficiency of *hlh-1(RNAi)*, we cannot rule out the possibility that other factor(s) may also contribute to the specification of BWM fate in the M lineage.

The synergistic loss of M-derived BWMs in *hlh-1(RNAi); fozi-1(cc609)* animals suggests functional overlap between FOZI-1 and HLH-1 in specifying BWM fate. However, each factor alone is clearly required for proper BWM fate specification, as *fozi-1* or *hlh-1* single mutants lack a small fraction of M-derived BWMs (Harfe et al., 1998a) (this work). Both *fozi-1* and *hlh-1* are expressed in the early M lineage as well as in the BWM and CC precursors at the time when these cell fates are specified (Harfe et al., 1998a) (this work). Although FOZI-1 is no longer detectable after these cells differentiate, HLH-1 continues to be expressed in differentiated BWM cells (Harfe et al., 1998a) (this work). We have shown that *fozi-1* and *hlh-1* do not regulate each other's expression and subcellular localization in the M lineage (Fig. 5). It is possible that in the M lineage, FOZI-1 and HLH-1 together contribute to process(es) required to specify BWM and CC fates that compete with an opposing process leading to SM fate specification. A slight shift in the balance between these two processes, as in *fozi-1* or *hlh-1* single mutants, can lead to transformation of the CC fate and loss of a fraction of M-derived BWMs. Loss of both FOZI-1 and HLH-1, however, shifts the balance strongly in favor of SMs. This interpretation requires that the M-derived CC fate is more sensitive than the BWM fate to the imbalance of these two opposing processes.

HLH-1 is a myogenic factor and has been shown to be capable of inducing widespread myogenesis when ectopically expressed during early embryogenesis (Fukushige and Krause, 2005). FOZI-1, however, does not appear to be a myogenic factor. Forced global expression of FOZI-1 did not lead to precocious myogenesis during embryogenesis, nor did it cause an SM to BWM fate transformation within the M lineage (data not shown, see Materials and methods for heat-shock conditions). The failure of FOZI-1 to induce myogenesis is not unexpected, as FOZI-1 is also expressed in a subset of head neurons and along the ventral nerve cord (Fig. 4E,F), and FOZI-1 has been shown to function in the specification of left-right asymmetric fates of the ASE neurons (Johnston et al., 2006). Thus FOZI-1 is required not only for the specification of striated BWM fates, but also for the specification of non-muscle cells such as CCs and ASE neurons. It is possible that different co-factors are required for FOZI-1 to exert its different functions in different cell types.

We believe that the Hox factor MAB-5 is one of the factors that function together with FOZI-1 in specifying the striated BWM fate in the M lineage. MAB-5 is present throughout the M lineage. *mab-5(0)* mutation results in multiple defects in the M lineage, including abnormal cleavage orientations, loss of expression of the CeTwist homolog HLH-8 in the early M lineage, and BWM and CC to SM fate transformations (S. J. Salser, PhD thesis, University of California, 1995) (Harfe et al., 1998b). We have shown that *fozi-*

1(cc609) mab-5(RNAi) animals behaved similarly to *fozi-1(cc609)* or *mab-5(0)* animals regarding BWM fate specification, whereas *hlh-1(cc561ts); mab-5(RNAi)*, like *hlh-1(cc561ts); fozi-1(cc609)* animals, exhibited synergistic loss of M-derived BWMs (Fig. 6A,B). As MAB-5 and FOZI-1 do not appear to regulate the expression of each other (Fig. 5E), our results suggest that MAB-5 and FOZI-1 function either together or in parallel in specifying M-derived BWM fate and that they do this by affecting a common downstream target that functions redundantly with HLH-1.

CEH-20 functions upstream of postembryonic myogenic pathways

Previous studies have shown that the homeodomain protein MLS-2 is required to activate the expression of HLH-1 in the M lineage and that *mls-2(0)* mutants have defects in BWM and CC fate specification (Jiang et al., 2005). We found that MLS-2 is not required for M lineage expression of FOZI-1, indicating that HLH-1 and FOZI-1 are regulated by different sets of transcription factors in the M lineage. We found that the Pbx/Exd homolog CEH-20 is required for the M lineage expression of FOZI-1 and that this regulation is independent of the Hox factor MAB-5 (Fig. 5). Interestingly, CEH-20 is also required for the expression of MLS-2 in the M lineage (Y. Jiang and J.L., unpublished). These observations place CEH-20 upstream of both HLH-1 and FOZI-1. As *ceh-20* mutant animals lack all M-derived BWMs (Liu and Fire, 2000), it is likely that any additional factors required for specifying M-derived BWM fate would also be downstream targets of CEH-20.

Based on all our results, we propose a model for how M-derived BWMs are specified, as depicted in Fig. 7. In this model, at least two redundant mechanisms are involved in specifying myogenic fates in the M lineage. First, MLS-2 regulates the expression of HLH-1, a myogenic factor. Second, FOZI-1 and MAB-5 regulate an unknown myogenic factor X that functions redundantly with HLH-1. At present, it is not clear whether MAB-5 functions together or in parallel with FOZI-1 in regulating factor X. Our data do not exclude the possibility of a third factor (Y) in addition to HLH-1 and factor X to promote myogenic fate specification. The Pbx/Exd homolog CEH-20 appears to act upstream of all of these myogenic pathways in the M lineage.

C. elegans embryonic and postembryonic myogenesis involve distinct mechanisms in addition to CeMyoD

The *C. elegans* striated musculature consists of 81 embryonically derived and 14 M lineage-derived BWMs (Sulston and Horvitz, 1977; Sulston et al., 1983). Despite their different lineage history, all 95 BWMs appear morphologically and functionally equivalent. It has been previously shown that although HLH-1 is sufficient to induce striated BWM fate (Fukushige and Krause, 2005), *hlh-1(0)* mutants still make all 81 embryonically derived BWMs (Chen et al., 1992; Chen et al., 1994). These studies suggest that other factors share redundant functions with HLH-1 in specifying these 81 BWMs. Neither FOZI-1 nor MAB-5 appears to be one of these factors, as FOZI-1 and MAB-5 are not expressed in the 81 embryonically derived BWMs or their precursors, and *fozi-1(cc609), mab-5(0)*, *hlh-1(cc561ts); fozi-1(cc609)*, *hlh-1(cc561ts); mab-5(RNAi)* and *hlh-1(cc561ts); fozi-1(cc609) mab-5(RNAi)* double and triple mutant animals do not have any defect in the specification of these 81 BWMs. Thus, although HLH-1 functions in the development of all BWMs, embryonic and postembryonic BWMs require distinct sets of transcription factors that function redundantly with HLH-1. Therefore there is a remarkable level of complexity for the production of a simple striated musculature in *C. elegans*.

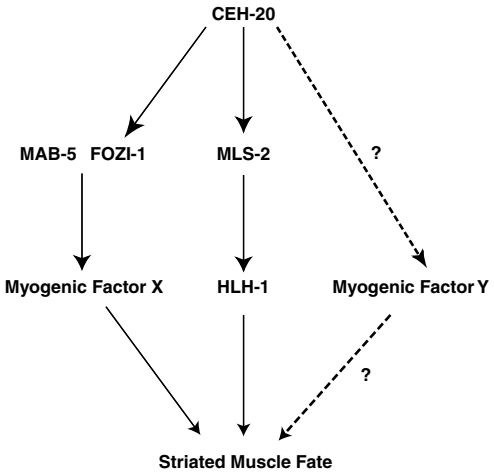

Fig. 7. A model for muscle fate specification in the postembryonic mesoderm. At least two redundant mechanisms functioning downstream of the Pbx/Exd homolog CEH-20 are involved in specifying myogenic fates in the postembryonic mesoderm (see Discussion). Solid lines in this model do not necessarily represent direct regulation. Dashed lines represent a hypothetical situation.

Functional redundancy in myogenic fate specification in vertebrates and invertebrates

Functional redundancy in specification of striated muscle fates has been observed in both vertebrates and invertebrates. In vertebrates, the redundancy is limited to proteins in the MyoD family. There are multiple members of the MyoD family of myogenic regulatory factors (MRFs) in vertebrates, including MyoD, Myf-5, myogenin and MRF4 (reviewed by Buckingham, 2001; Pownall et al., 2002; Buckingham et al., 2003). Each of these factors is capable of inducing the transcription of muscle-specific genes when overexpressed, but they also share functional redundancy in striated muscle development (reviewed by Pownall et al., 2002). For example, mice lacking either Myf-5 or MyoD are viable and fertile (Braun et al., 1992; Rudnicki et al., 1992; Kaul et al., 2000). However, double mutants lacking both Myf-5 and MyoD do not form any skeletal muscles (Rudnicki et al., 1993).

Different from vertebrates, many invertebrate organisms have only one MyoD homolog, including ascidians (*AMD-1*) (Araki et al., 1994), sea urchins (*sum-1*) (Venuti et al., 1991) and *Drosophila* (*nautilus*) (Michelson et al., 1990). In *Drosophila*, *nautilus* is present in a subset of muscle precursors and differentiated muscle fibers (Michelson et al., 1990; Paterson et al., 1991). *nautilus* loss-of-function mutants have defects in only a distinct subset of cells normally expressing *nautilus*, and the defects appear to be a combination of abnormal differentiation of some muscle fibers and inappropriate fate specification (Keller et al., 1998; Balagopalan et al., 2001). These observations indicate that there are factor(s) functioning redundantly with *nautilus* in muscle fate specification and differentiation. The identity of these factors is currently unknown. It is possible that some of the muscle identity genes such as *slouch, apterous, muscle segment homeobox, ladybird* and *Krüppel* (Baylies et al., 1998; Frasch, 1999) could share redundant functions with *nautilus* in specifying the fate of certain muscle fibers.

Our work shows that the combinatorial functions of HLH-1 with FOZI-1 and MAB-5 are required to specify the M-derived BWM fate. This is similar to the situation in *Drosophila*, in which unique combinations of different muscle identity genes specify distinct muscle fiber fates, and loss-of-function mutations in these genes

cause fate transformation from one type of muscle fiber to another (Bourgouin et al., 1992; Ruiz-Gomez et al., 1997; Jagla et al., 1998; Nose et al., 1998; Knirr et al., 1999). Notably, both MAB-5 and FOZI-1 are expressed in other cell types outside of the M lineage in *C. elegans* (S. J. Salser, PhD thesis, University of California, 1995; this work). The expression pattern of muscle identity genes in *Drosophila* is also not restricted only to muscle cells (Bourgouin et al., 1992; Jagla et al., 1998; Nose et al., 1998; Knirr et al., 1999). What is unique in our study is that *hlh-1(cc561ts); mab-5(RNAi)* and *hlh-1(cc561ts); fozi-1(cc609)* animals show clear fate transformations from M-derived BWMs to non-muscle SM-like cells, which not only display the morphology of SMs, but also go on to proliferate and produce differentiated non-striated sex muscles. This muscle to non-muscle fate transformation may be due to these cells adopting a developmental ground state represented by the SMs when myogenic factors are missing from the M lineage.

Supplementary material

Supplementary material for this article is available at http://dev.biologists.org/cgi/content/full/134/1/19/DC1

We thank Marisa Foehr for repeating the RNAi experiments to confirm the identity of *fozi-1*; Mike Krause, Yuji Kohara, Shohei Mitani and the Sanger Center for *C. elegans* strains, cosmids, cDNA clones and antibodies; Marisa Foehr, Yuan Jiang, Ken Kemphues, Siu Sylvia Lee and Diane Morton for helpful discussions, suggestions and valuable comments on the manuscript. J.L. appreciates the advice and support of Andy Fire, in whose lab the *fozi-1* mutants were isolated. Some strains used in this study were obtained from the *C. elegans* Genetics Center (CGC), which is supported by a grant from the NIH National Center for Research Resources. This work was supported by NIH R01 GM066953 (to J.L.) and GM39066 (to D.P. and A.B.). During part of this work, N.M.A. was supported by NIH T32 GM07617 and a GAANN fellowship sponsored by the U.S. Department of Education. D.T. was supported by the Summer Research Fellowship from Weill Cornell Medical College in Qatar.

References

Araki, I., Saiga, H., Makabe, K. W. and Sato, N. (1994). Expression of AMD1, a gene for a MyoD1-related factor in the Ascidian Halocynthia Roretzi. *Roux's Arch. Develop. Biol.* **203**, 320-327.

Balagopalan, L., Keller, C. A. and Abmayr, S. M. (2001). Loss-of-function mutations reveal that the Drosophila nautilus gene is not essential for embryonic myogenesis or viability. *Dev. Biol.* **231**, 374-382.

Baylies, M. K., Bate, M. and Ruiz Gomez, M. (1998). Myogenesis: a view from Drosophila. *Cell* **93**, 921-927.

Bourgouin, C., Lundgren, S. E. and Thomas, J. B. (1992). Apterous is a Drosophila LIM domain gene required for the development of a subset of embryonic muscles. *Neuron* **9**, 549-561.

Braun, T., Rudnicki, M. A., Arnold, H. H. and Jaenisch, R. (1992). Targeted inactivation of the muscle regulatory gene myf-5 results in abnormal rib development and perinatal death. *Cell* **71**, 369-382.

Brenner, S. (1974). The genetics of *Caenorhabditis elegans*. *Genetics* **77**, 71-94.

Bretscher, A. (1981). Fimbrin is a cytoskeletal protein that crosslinks F-Actin in vitro. *Proc. Natl. Acad. Sci. USA* **78**, 6849-6853.

Buckingham, M. (2001). Skeletal muscle formation in vertebrates. *Curr. Opin. Genet. Dev.* **11**, 440-448.

Buckingham, M., Bajard, L., Chang, T., Daubas, P., Hadchouel, J., Meilhac, S., Montarras, D., Rocancourt, D. and Relaix, F. (2003). The formation of skeletal muscle: from somite to limb. *J. Anat.* **202**, 59-68.

Chen, L., Krause, M., Draper, B., Weintraub, H. and Fire, A. (1992). Body-wall muscle formation in *Caenorhabditis elegans* embryos that lack the MyoD homolog Hlh-1. *Science* **256**, 240-243.

Chen, L., Krause, M., Sepanski, M. and Fire, A. (1994). The *Caenorhabditis elegans* MyoD homologue HLH-1 is essential for proper muscle function and complete morphogenesis. *Development* **120**, 1631-1641.

Corsi, A. K., Kostas, S. A., Fire, A. and Krause, M. (2000). *Caenorhabditis elegans* Twist plays an essential role in non-striated muscle development. *Development* **127**, 2041-2051.

Fire, A., Xu, S., Montgomery, M. K., Kostas, S. A., Driver, S. E. and Mello, C. C. (1998). Potent and specific genetic interference by double-stranded RNA in *Caenorhabditis elegans*. *Nature* **391**, 806-811.

Foehr, M. L., Lindy, A. S., Fairbank, R. C., Amin, N. M., Xu, M., Yanowitz, J., Fire, A. Z. and Liu, J. (2006). An antagonistic role for the *C. elegans* Schnurri homolog SMA-9 in modulating TGFbeta signaling during mesodermal patterning. *Development* **133**, 2887-2896.

Frasch, M. (1999). Controls in patterning and diversification of somatic muscles during Drosophila embryogenesis. *Curr. Opin. Genet. Dev.* **9**, 522-529.

Fukushige, T. and Krause, M. (2005). The myogenic potency of HLH-1 reveals wide-spread developmental plasticity in early *C. elegans* embryos. *Development* **132**, 1795-1805.

Harfe, B. D., Branda, C. S., Krause, M., Stern, M. J. and Fire, A. (1998a). MyoD and the specification of muscle and non-muscle fates during postembryonic development of the *C. elegans* mesoderm. *Development* **125**, 2479-2488.

Harfe, B. D., Vaz Gomes, A., Kenyon, C., Liu, J., Krause, M. and Fire, A. (1998b). Analysis of a *Caenorhabditis elegans* Twist homolog identifies conserved and divergent aspects of mesodermal patterning. *Genes Dev.* **12**, 2623-2635.

Harris, E. S., Li, F. and Higgs, H. N. (2004). The mouse Formin, FRLalpha, slows actin filament barbed end elongation, competes with capping protein, accelerates polymerization from monomers, and severs filaments. *J. Biol. Chem.* **279**, 20076-20087.

Higgs, H. N. and Peterson, K. J. (2005). Phylogenetic analysis of the Formin homology 2 domain. *Mol. Biol. Cell* **16**, 1-13.

Hodgkin, J. and Doniach, T. (1997). Natural variation and copulatory plug formation in *Caenorhabditis elegans*. *Genetics* **146**,149-164.

Hodgkin, J., Horvitz, H. R. and Brenner, S. (1979). Nondisjunction mutants of the nematode *Caenorhabditis elegans*. *Genetics* **91**, 67-94.

Hurd, D. D. and Kemphues, K. J. (2003). PAR-1 is required for morphogenesis of the *Caenorhabditis elegans* vulva. *Dev. Biol.* **253**, 54-65.

Iuchi, S. (2001). Three classes of C2H2 zinc finger proteins. *Cell Mol. Life Sci.* **58**, 625-635.

Jagla, T., Bellard, F., Lutz, Y., Dretzen, G., Bellard, M. and Jagla, K. (1998). Ladybird determines cell fate decisions during diversification of Drosophila somatic muscles. *Development* **125**, 3699-3708.

Jiang, Y., Horner, V. and Liu, J. (2005). The HMX homeodomain protein MLS-2 regulates cleavage orientation, cell proliferation and cell fate specification in the *C. elegans* postembryonic mesoderm. *Development* **132**, 4119-4130.

Johnston, R. J., Jr, Copeland, J. W., Fasnacht, M., Etchberger, J. F., Liu, J., Honig, B. and Hobert, O. (2006). An unusual Zn-finger/FH2 domain protein controls a left/right asymmetric neuronal fate decision in *C. elegans*. *Development* **133**, 3317-3328.

Kaul, A., Koster, M., Neuhaus, H. and Braun, T. (2000). Myf-5 revisited: loss of early myotome formation does not lead to a rib phenotype in homozygous *Myf-5* mutant mice. *Cell* **102**, 17-19.

Keller, C. A., Grill, M. A. and Abmayr, S. M. (1998). A role for nautilus in the differentiation of muscle precursors. *Dev. Biol.* **202**, 157-171.

Kenyon, C. (1986). A gene involved in the development of the posterior body region of *C. elegans*. *Cell* **46**, 477-487.

Knirr, S., Azpiazu, N. and Frasch, M. (1999). The role of the NK-homeobox gene slouch (S59) in somatic muscle patterning. *Development* **126**, 4525-4535.

Kostas, S. A. and Fire, A. (2002). The T-box factor MLS-1 acts as a molecular switch during specification of nonstriated muscle in *C. elegans*. *Genes Dev.* **16**, 257-269.

Kovar, D. R., Kuhn, J. R., Tichy, A. L. and Pollard, T. D. (2003). The fission yeast cytokinesis formin Cdc12p is a barbed end actin filament capping protein gated by profilin. *J. Cell Biol.* **161**, 875-887.

Krause, M., Fire, A., Harrison, S. W., Priess, J. and Weintraub, H. (1990). CeMyoD accumulation defines the body wall muscle cell fate during *C. elegans* embryogenesis. *Cell* **63**, 907-919.

Liu, J. and Fire, A. (2000). Overlapping roles of two Hox genes and the Exd ortholog ceh-20 in diversification of the *C. elegans* postembryonic mesoderm. *Development* **127**, 5179-5190.

Maeda, I., Kohara, Y., Yamamoto, M. and Sugimoto, A. (2001). Large-scale analysis of gene function in *Caenorhabditis elegans* by high-throughput RNAi. *Curr. Biol.* **11**, 171-176.

Matsuzaki, Y., Fujisawa, J. and Yoshida, M. (1995). Identification of transcriptional activation domain of TREB5, a CREB/ATF family protein that binds to HTLV-1 enhancer. *J. Biochem. (Tokyo)* **117**, 303-308.

Mello, C. C., Kramer, J. M., Stinchcomb, D. and Ambros, V. (1991). Efficient gene transfer in *C. elegans*: extrachromosomal maintenance and integration of transforming sequences. *EMBO J.* **10**, 3959-3970.

Michelot, A., Guerin, C., Huang, S., Ingouff, M., Richard, S., Rodiuc, N., Staiger, C. J. and Blanchoin, L. (2005). The formin homology 1 domain modulates the actin nucleation and bundling activity of Arabidopsis FORMIN1. *Plant Cell* **17**, 2296-2313.

Michelson, A. M., Abmayr, S. M., Bate, M., Arias, A. M. and Maniatis, T. (1990). Expression of a MyoD family member prefigures muscle pattern in Drosophila embryos. *Genes Dev.* **4**, 2086-2097.

Moseley, J. B. and Goode, B. L. (2005). Differential activities and regulation of *Saccharomyces cerevisiae* formin proteins Bni1 and Bnr1 by Bud6. *J. Biol. Chem.* **280**, 28023-28033.

Nose, A., Isshiki, T. and Takeichi, M. (1998). Regional specification of muscle progenitors in Drosophila: the role of the Msh homeobox gene. *Development* **125**, 215-223.

Olmsted, J. B. (1981). Affinity purification of antibodies from diazotized paper blots of heterogeneous protein samples. *J. Biol. Chem.* **256**, 11955-11957.
Paterson, B. M., Walldorf, U., Eldridge, J., Dubendorfer, A., Frasch, M. and Gehring, W. J. (1991). The Drosophila homologue of vertebrate myogenic-determination genes encodes a transiently expressed nuclear protein marking primary myogenic cells. *Proc. Natl. Acad. Sci. USA* **88**, 3782-3786.
Pollard, T. D. (1983). Measurement of rate constants for actin filament elongation in solution. *Anal. Biochem.* **134**, 406-412.
Pownall, M. E., Gustafsson, M. K. and Emerson, C. P., Jr (2002). Myogenic regulatory factors and the specification of muscle progenitors in vertebrate embryos. *Annu. Rev. Cell Dev. Biol.* **18**, 747-783.
Pruyne, D., Evangelista, M., Yang, C., Bi, E., Zigmond, S., Bretscher, A. and Boone, C. (2002). Role of formins in actin assembly: nucleation and barbed-end association. *Science* **297**, 612-615.
Rudnicki, M. A., Braun, T., Hinuma, S. and Jaenisch, R. (1992). Inactivation of MyoD in mice leads to up-regulation of the myogenic HLH gene Myf-5 and results in apparently normal muscle development. *Cell* **71**, 383-390.
Rudnicki, M. A., Schnegelsberg, P. N., Stead, R. H., Braun, T., Arnold, H. H. and Jaenisch, R. (1993). MyoD or Myf-5 is required for the formation of skeletal muscle. *Cell* **75**, 1351-1359.
Ruiz-Gomez, M., Romani, S., Hartmann, C., Jackle, H. and Bate, M. (1997). Specific muscle identities are regulated by Kruppel during Drosophila embryogenesis. *Development* **124**, 3407-3414.
Sagot, I., Rodal, A. A., Moseley, J., Goode, B. L. and Pellman, D. (2002). An actin nucleation mechanism mediated by Bni1 and profilin. *Nat. Cell Biol.* **4**, 626-631.
Smith, D. B. and Johnson, K. S. (1988). Single-step purification of polypeptides expressed in *Escherichia coli* as fusions with Glutathione S-transferase. *Gene* **67**, 31-40.
Smith, D. E. and Fisher, P. A. (1984). Identification, developmental regulation, and response to heat shock of two antigenically related forms of a Mm nuclear envelope protein in Drosophila embryos: application of an improved method for affinity purification of antibodies using polypeptides immobilized on nitrocellulose blots. *J. Cell Biol.* **99**, 20-28.
Stepchenko, A. and Nirenberg, M. (2004). Mapping activation and repression domains of the vnd/NK-2 homeodomain protein. *Proc. Natl. Acad. Sci. USA* **101**, 13180-13185.
Sulston, J. E. and Horvitz, H. R. (1977). Post-embryonic cell lineages of the nematode *Caenorhabditis elegans*. *Dev. Biol.* **56**, 110-156.
Sulston, J. E., Schierenberg, E., White, J. G. and Thomson, J. N. (1983). The embryonic cell lineage of the nematode *Caenorhabditis elegans*. *Dev. Biol.* **100**, 64-119.
Venuti, J. M., Goldberg, L., Chakraborty, T., Olson, E. N. and Klein, W. H. (1991). A myogenic factor from Sea urchin embryos capable of programming muscle differentiation in mammalian cells. *Proc. Natl. Acad. Sci. USA* **88**, 6219-6223.
Wicks, S. R., Yeh, R. T., Gish, W. R., Waterston, R. H. and Plasterk, R. H. (2001). Rapid gene mapping in *Caenorhabditis elegans* using a high density polymorphism map. *Nat. Genet.* **28**, 160-164.
Xu, Y., Moseley, J. B., Sagot, I., Poy, F., Pellman, D., Goode, B. L. and Eck, M. J. (2004). Crystal structures of a Formin homology-2 domain reveal a tethered dimer architecture. *Cell* **116**, 711-723.
Yang, L., Sym, M. and Kenyon, C. (2005). The roles of two *C. elegans* HOX co-factor orthologs in cell migration and vulva development. *Development* **132**, 1413-1428.
Zigmond, S. H., Evangelista, M., Boone, C., Yang, C., Dar, A. C., Sicheri, F., Forkey, J. and Pring, M. (2003). Formin leaky cap allows elongation in the presence of tight capping proteins. *Curr. Biol.* **13**, 1820-1823.